SOCIETY FOR SCIENCE AND EDUCATION
UNITED KINGDOM
TMLAI TRANSACTIONS ON MACHINE LEARNING AND ARTIFICIAL INTELLIGENCE
VOLUME 5 NO 4, 2017
ISSN 2054-7390

Comparative Study of Exact Continuous Orthogonal Moments Applications : Local Feature Extraction and Data Compression

Zaineb Bahaoui[1] , Rachid Benouini[1], Hakim EL Fadili[2], Khalid Zenkouar[3], Arsalane Zarghili[3]
[1]Laboratoire Systèmes Intelligents & Applications (LSIA), Faculty of Science Technique Fes, Université Sidi Mohamed Ben Abdellah. Fes Morocco.
[1]Laboratoire Systèmes Intelligents & Applications (LSIA), Faculty of Science Technique Fes,
[2]Laboratoire LIPI (Informatique et Physique Interdisciplinaire),ENSA School, Université Sidi Mohamed Ben Abdellah, Fes Morocco
z.bahaoui@gmail.com

ABSTRACT

This paper present an improved reconstruction algorithm of the multi-gray level images based on overlapping block method using exact continuous moments computation: Legendre , Zernike, Pseudo-Zernike and Gegenbauer moments . We solve the artifact issue caused by unitary block reconstruction which affects the visual image quality. This method aim to ensure high accuracy and low computation time, using only small finite number of moments. Our approaches aims to introduce these moments in the field of data compression and local feature extraction for pattern recognition. Experimental results show the superiority of our proposed approaches over the existing methods.

Keywords-Exact continuous moments; Legendre moments, Zernike moments; Pseudo-Zernike moments; Gegenbauer moments; Overlapping block ; Feature extraction; Compression.

1 Introduction

Since the introduction of Hu's moment methods in 1962 [1], the moments functions have been used extensively in many research fields, especially in the fields of image processing and pattern recognition, thanks to the unique global features of moment description [2-7].

As Legendre, Zernike, Pseudo-Zernike and Gegenbauer moments use the continuous orthogonal polynomials as a basis functions. They all offer a better representation capacity and increases robustness to image noise over other types of moments [2-3]. Yet they suffer from a lack of accuracy, especially due to numerical approximation errors. In order to reduce those errors, many recent works proposed a set of exact computation algorithms [8-12].

Globally, the computation of continuous moments is a time consuming procedure, mostly because of two reasons: First, the handling of a set of complicated entities for each moments order. Also, the use of great reconstruction space, involve a huge quantity of information, using high moments orders [13-15].

On the other hand, researchers have been working on establishing the mathematical formulas to describe the relationship between the global and local moment features within the same image. In this regard, we suggest a novel approach offering fast and efficient reconstruction algorithm in the case

DOI: 10.14738/tmlai.54.3226
Publication Date: 15th August, 2017
URL: http://dx.doi.org/10.14738/tmlai.54.3226

of multi-gray level images with greater sizes, concentrating on the local feature extraction. Our main objective is to reach high reconstruction quality using only a small finite number of moments, by splitting the original image into blocks, and using fast and exact approximation. This strategy relies in the utilization of low-order polynomials on small intervals instead of high orders on a single one [13]. This aims to introduce these continues moments in the data compression field, which can be achieved by transforming the data, projecting them on the basis of functions, and then encoding the resulted coefficients [16-17]. Therefore, the input image is partitioned into blocks of pixels which are then reconstructed as separate entities.

This novel methodology based on a decomposition technique enables fast computation of image moments. Such a process is commonly used in image compression standards, e.g. in JPEG [18] where image is partitioned into blocks and DCT coefficients are computed in each part

However, when adjacent blocks have different reconstruction values, the block boundaries become visible, producing vertical and horizontal lines in the reconstructed images. This phenomenon is known as the blocking artifact [19].

To deal with this issue, we propose a new Overlapping concept, which use the neighboring information of each block and exploits the inter-block correlation. This new approach called Overlapping Block based Reconstruction (OBR), has been implemented with four different Exact continuous Moments types: Legendre (OBRELM), Zernike (OBREZM), Pseudo-Zernike(OBREPZM) and Gegenbauer (OBREGM).

In order to evaluate the performances of those four new methods, we performed a set of comparative tests on a multi-gray level images, in terms of local feature extraction either in visual quality, in PSNR or in SSIM index [20].In addition, a comparison has been conducted between a reference method, DCT, and our four proposed methods, in order to investigate whether this continuous moments an provide an alternative to the existing JPEG compression.

The rest of the paper is organized as follows. Section 2, describes the recently introduced Exact Moments computation. In section 3 we point out the theoretical details of the proposed OBRELM, OBREZM and OBREGM methods. We describe the two application of our algorithm in section 4. Finally, Section 5 gives the experimental validation with the summary of important results, and concluding remarks are presented in section 6.

2 Exactcontinuousmoments computation

2.1 Exact Legendre moments (ELM)

The $(p+q)$ order Exact Legendre Moments (ELM) [8-9], of an $M \times N$ image described by its intensity function $f(x,y)$ is:

$$L^{E}{}_{p,q} = \sum_{1}^{M}\sum_{1}^{N} I_p(x_i)\, I_q(y_j) f(x_i, y_j), \tag{1}$$

where

$$\begin{aligned} I_p(x_i) &= \tfrac{2p+1}{2}\textstyle\int_{U_i}^{U_{i+1}} P_p(x)dx/ \\ I_q(y_j) &= \tfrac{2q+1}{2}\textstyle\int_{V_j}^{V_{j+1}} P_q(y)d\ y, \end{aligned} \tag{2}$$

And

$$\int P_p(x)dx = \frac{P_{p+1}(x)-P_{p-1}(x)}{2p+1}/ \qquad (3)$$
$$\int P_q(y)dy = \frac{P_{q+1}(y)-P_{q-1}(y)}{2q+1}.$$

For the computation of Legendre polynomials, the recurrence relation can be used [8]:

$$P_{p+1}(x) = \frac{(2p+1)}{(p+1)}xP_p(x) - \frac{P}{(p+1)}P_{p-1}(x). \qquad (4)$$

For simplicity, upper and lower limits of the integration in (2) and (3) will be expressed as follows:

$$U_{i+1} = -1 + i\Delta x, U_i = -1 + (i-1)\Delta x. \qquad (5)$$

Similarly,

$$V_{j+1} = -1 + j\Delta y, V_j = -1 + (j-1)\Delta y. \qquad (6)$$

Using (2), (3) and (4), the integral parts will be written as follows:

$$\int_{U_i}^{U_{i+1}} P_p(x)dx = \left[\frac{P_{p+1}(x)-P_{p-1}(x)}{2p+1}\right]_{U_i}^{U_{i+1}}/ \qquad (7)$$
$$\int_{V_j}^{V_{j+1}} P_q(y)dx = \left[\frac{P_{q+1}(y)-P_{q-1}(y)}{2q+1}\right]_{V_j}^{V_{j+1}}.$$

Substitute $P_{p+1}(x)$ from (4) into (7) yields (8):

$$\int_{U_i}^{U_{i+1}} P_p(x)dx = \frac{1}{p+1}\left[xP_{p+1}(x) - P_{p-1}(x)\right]_{U_i}^{U_{i+1}} / \int_{V_j}^{V_{j+1}} P_q(y)dy = \frac{1}{q+1}\left[yP_{q+1}(y) - P_{q-1}(y)\right]_{V_j}^{V_{j+1}}. \qquad (8)$$

The set of Legendre moments can thus be computed exactly by (1) where

$$I_p(x_i) = \frac{2p+1}{2p+2}\left[xP_{p+1}(x) - P_{p-1}(x)\right]_{U_i}^{U_{i+1}} /$$
$$I_q(y_j) = \frac{2q+1}{2q+2}\left[yP_{q+1}(y) - P_{q-1}(y)\right]_{V_j}^{V_{j+1}}. \qquad (9)$$

Equation (1) is called the exact computation of Legendre moments (ELM) [8-9].

The image function $f(x,y)$ can be written as an infinite series of expansion in terms of the Legendre polynomials over the square $[-1,1]$

$$f(x,y) = \sum_{p=0}^{\infty}\sum_{q=0}^{\infty} L_{p,q}\ P_p(x)\,P_q(y), \qquad (10)$$

where the Legendre moments $L^E_{p,q}$ are computed over the same square. If only Legendre moments of order $p+q \leq max$ are given, then the function $f(x,y)$ can be approximated by a truncated finite series :

$$\hat{f}_{max}(x,y) = \sum_{p=0}^{max}\sum_{q=0}^{p} L_{p-q,q}P_{p-q}(x)P_q(y), \qquad (11)$$

where the number of moments used in this form for image reconstruction is defined by [3]:

$$N_{total} = \frac{(max+1)(max+2)}{2}. \qquad (12)$$

2.2 Exact Zernike moments (EZM)

Exact Zernike moments are computed by using exact geometric moments, proposed by Hosny in [10]. The approach by first calculating the geometric moments accurately, then employing the relationship in (13)of Zernike moments and the geometric moments.

$$Z_{pq} = \frac{p+1}{\pi} \sum_{\substack{k=|q| \\ p-k=even}}^{p} \sum_{j=0}^{s} \sum_{m=0}^{|q|} w^m \binom{s}{j} \binom{|q|}{m} B_{p|q|k} G_{k-2j-m,\ 2j+m}, \tag{13}$$

where$s = 0.5(k - |q|)$ and $\hat{\imath} = \sqrt{-1}$

$$w = \begin{cases} -\hat{\imath}, & q > 0 \\ \hat{\imath}, & q \leq 0 \end{cases}, \tag{14}$$

The Exact Zernike moments$Z_{pq}^{E}$is simplified as following:

$$Z_{pq}^{E} = \frac{p+1}{\pi} \sum_{\substack{k=|q| \\ p-k=even}}^{p-2} B_{p|q|k} Rad_{kq} \tag{15}$$

Zernike polynomial coefficients are computed using the following recurrence relations:

$$B_{ppp} = 1, \tag{16}$$

$$B_{p(q-2)p} = \frac{p+q}{p-q+2} B_{pqp}, \tag{17}$$

$$B_{pq(k-2)} = \frac{(k+q)(k-q)}{(p+k)(p-k+2)} B_{pqk}. \tag{18}$$

The time consuming direct computations of factorial terms are avoided by using the following recurrence relations:

$$D(p,k) = \frac{p+q}{p-k} D(p-1,k), \tag{19}$$

$$D(p,k) = \frac{1}{k(p-k)} D(p,k-1), \tag{20}$$

with$D(0,0) = 1$,and $D(p,0) = 1$.

The radial Zernike moments are expressed as a combination of geometric moments.

$$Rad_{kq} = \sum_{j=0}^{s} \sum_{m=0}^{|q|} w^m D(s,j) D(q,m) G_{k-2j-m,\ 2j+m}. \tag{21}$$

Hosny in [46] proposed an exact and fast geometric moments's computation. In this exact method, the set of geometric moments can thus be computed exactly by:

$$G_{pq} = \sum_{i=0}^{N} \sum_{j=0}^{N} I_p(i) I_q(j)\, f(x_i, y_j), \tag{22}$$

where

$$I_p(i) = \frac{1}{p+1} \left[U_{i+1}^{p+1} - U_i^{p+1} \right] / \\ I_q(j) = \frac{1}{q+1} \left[U_{j+1}^{q+1} - U_j^{q+1} \right], \tag{23}$$

Fast computation of exact geometric moments can be achieved by successive computation of the qth order moments for each row. (22)will be rewritten in a separable form as follows:

$$G_{pq} = \sum_{i=0}^{N} I_p(i) Y_{iq}(j). \tag{24}$$

where

$$Y_{iq} = \sum_{j=0}^{N} I_q(j) f(x_i, y_j). \tag{25}$$

Y_{iq}in(25)is the q^{th} order moments of row i. Since,$I_0(i) = \frac{\sqrt{2}}{N}$.

Substitute $I_0(i)$ into (23) yields;

$$G_{0q} = \frac{\sqrt{2}}{N} \sum_{i=0}^{N} Y_{iq}(j). \tag{26}$$

The image intensity function $f(x, y)$ can then be expressed in terms of Zernike polynomials over the unit circle as

$$f(x,y) = \sum_{p=0}^{\infty} \sum_{\substack{q \\ p-q=even \\ q \le p}} \lambda_p Z_{pq} V_{pq}(x,y), \tag{27}$$

whereλ_p is a normalization constant that depends on the square to circular mapping technique and

$$V_{pq}(x,y) = R_{pq}(r) e^{-iq\theta}, r \in [-1,1] \tag{28}$$

Where $r = \sqrt{x^2 + y^2}$ is the length of the vector from the origin to the pixel (x, y), and $\theta = \tan^{-1}(y/x)$ is the angle between the vector r and the principle x-axis. The real valued radial polynomials are given by

$$R_{pq}(r) = \sum_{\substack{k=q \\ p-k=even}}^{p} B_{p|q|k} r^k, \tag{29}$$

where the polynomial coefficients, $B_{p|q|k}$ are defined as:

$$B_{p|q|k} = \frac{(-1)^{\left(\frac{p-k}{2}\right)} \left(\frac{p+k}{2}\right)!}{\left(\frac{p-k}{2}\right)! \left(\frac{k+q}{2}\right)! \left(\frac{k-q}{2}\right)!}, \tag{30}$$

With Zernike moments,Z_{pq} are computed over the same unit circle. However, the reconstruction of image function using arbitrary large order of Zernike moments is not efficient. Therefore, this series expansion is truncated at a finite order, Max, and considered as optimum approximation to the original image function. The reconstructed image intensity function$\hat{f}(x, y)$, based on the truncated series, is given as:

$$\hat{f}_{Max}(x,y) \approx \sum_{p=0}^{Max} \sum_{\substack{q \\ p-q=even \\ q \le p}}^{p} \lambda_p Z_{pq} V_{pq}(x,y). \tag{31}$$

Where the number of moments used in this form for image reconstruction is definedin [3] by:

$$N_{total} = \begin{cases} (\frac{Max+2}{2})^2, & Maxiseven \\ (\frac{Max+1}{2})^2 + \frac{Max+1}{2}, & Maxisodd \end{cases} \quad (32)$$

2.3 Exact Pseudo-Zernike moments (EPZM)

EPZM are computed as a linear combination of exact geometric and radial geometric moments, where they are exactly computed by using mathematical integration [11].

$$PZ_{pq} = \frac{p+1}{\pi} \left(\sum_{\substack{k=q \\ k-q=even}}^{p} B_{p;q;k} R^{G}_{k,q} + \sum_{\substack{k=q+1 \\ k-q=odd}}^{p} B_{p;q;k} R^{H}_{k,q} \right), \quad (33)$$

where

$$R^{G}_{k,q} = \sum_{j=0}^{s} \sum_{m=0}^{q} (-\hat{\imath})^m C_j^S C_m^q GM_{k-2j-m,\ 2j+m}, \quad (34)$$

$$R^{H}_{k,q} = \sum_{j=0}^{s} \sum_{m=0}^{q} (-\hat{\imath})^m C_j^S C_m^q H_{k-2j-m,\ 2j+m}. \quad (35)$$

The PZM coefficients B_{pqk} are computed using the following recurrence relations:

$$B_{ppp} = 1, \quad (36)$$

$$B_{p(q-1)p} = \frac{k+p+1}{p-q+1} B_{pqp}, \quad (37)$$

$$B_{pq(k-1)} = \frac{(k+q+1)(k-q)}{(p+k+1)(p-k+1)} B_{pqk}. \quad (38)$$

The geometric and radial geometric moments GM_{pq} and H_{pq} are defined in function, of image intensity $f(x,y)$, as follows:

$$GM_{pq} = \sum_{i=0}^{[\frac{N}{2}]} \sum_{j=0}^{[\frac{N}{2}]} I_p(i) I_q(j) f(x_i, y_j), \quad (39)$$

$$H_{pq} = \sum_{i=0}^{[\frac{N}{2}]} \sum_{j=0}^{[\frac{N}{2}]} I_p(i) I_q(j) \sqrt{x^2+y^2} f(x_i, y_j), \quad (40)$$

where $I_p(x)$ and $I_q(y)$ are calculated by Eq.(23).

Where the number of moments used in this form for image reconstruction is defined in [3] by:

$$N_{total} = (Max+1)^2 \quad (41)$$

2.4 Exact Gegenbauer moments (EGM)

The accurate orthogonal Gegenbauer moments of order *(p, q)* [12] with the scaling parameter $\alpha > -0.5$ are defined as follows:

$$G^{(\alpha)}_{p,q} = \frac{1}{C_p(\alpha) C_q(\alpha)} \sum_{1}^{M} \sum_{1}^{N} IX_p(x_i)\, IY_q(y_j) f(x_i, y_j), \quad (42)$$

where the normalization constant $C_p(\alpha)$ defined with the recurrence relation as:

$$C_p(\alpha) = \frac{(p-1+\alpha)(p-1+2\alpha)}{p(p+\alpha)} C_{p-1}(\alpha) \tag{43}$$

$$C_0(\alpha) = \frac{\pi\Gamma(2\alpha)}{2^{2\alpha-1}\alpha[\Gamma(\alpha)]^2}$$

The symbol, Γ(.), refers to gamma function and:

$$IX_p(x_i) = \sum_{k=0}^{[\frac{p}{2}]} B_{p,k}^{(\alpha)} I_{p-2k}(x_i) \tag{45}$$

$$IY_q(y_j) = \sum_{k=0}^{[\frac{q}{2}]} B_{q,k}^{(\alpha)} I_{q-2k}(y_j) \tag{46}$$

The floor operator $[p/2]$, equal to either $(p-1)/2$ or $p/2$ for odd and even values of p, and the coefficients matrix $B_{p,k}^{(\alpha)}$ obey the following recursive relations

$$B_{0,0}^{(\alpha)} = 1, \tag{47}$$

$$B_{p,0}^{(\alpha)} = \frac{2(\alpha+p-1)}{p} B_{p-1,0}^{(\alpha)}, \tag{48}$$

$$B_{p,k}^{(\alpha)} = \frac{(p-2k+2)(p-2k+1)}{4k(\alpha+p-k)} B_{p,k-1}^{(\alpha)}, \tag{49}$$

The definite integration $I_{p-2k}(x_i)$and $I_{q-2k}(y_j)$ is evaluated using the recurrence relation:

$$I_T = \frac{1}{(2\alpha+T)}[U_i^{T-1}(1-U_i^2)^{\alpha+0.5} - U_{i+1}^{T-1}(1-U_{i+1}^2)^{\alpha+0.5} + (T-1)I_{T-2} \tag{50}$$

where$T$ is a non-negative integer, $T = 2, 3, 4, \ldots..Max$,with Max is the maximum order of Gegenbauer moments, and $I_0 = \int_{U_i}^{U_{i+1}} (1-x^2)^{\alpha-0.5} dx$ and $I_1 = \frac{1}{(2\alpha+1)}[(1-U_i^2)^{\alpha+0.5} - (1-U_{i+1}^2)^{\alpha+0.5}]$.

The integration of I_0 is difficult to be evaluated analytically. So, an accurate numerical integration method is a good choice. The composite Simpson's rule is proved to be very accurate where the numerical and exact values are almost equal [12].

For the computation of Gegenbauer polynomials, the recurrence relation can be used :

$$P_{p+1}^{(\alpha)}(x) = \frac{(2p+2\alpha)}{(p+2\alpha)} x P_p^{(\alpha)}(x) - \frac{p+2\alpha-1}{(p+1)} P_{p-1}^{(\alpha)}(x) \tag{51}$$

with$P_0^{(\alpha)}(x) = 1$, $P_1^{(\alpha)}(x) = 2\alpha x$ and $p \geq 0$.

The image function $f(x,y)$ can be written as an infinite expansion series in terms of the Gegenbauer polynomials over the square$[-1,1]x\ [-1,1]$:

$$f(x,y) = \sum_{p=0}^{\infty} \sum_{q=0}^{\infty} G_{p,q}^{(\alpha)} P_p^{(\alpha)}(x) P_q^{(\alpha)}(y) \tag{52}$$

where the Gegenbauer moments, $G_{p,q}^{(\alpha)}$, are computed over the same square. If only Gegenbauer moments of order smaller than or equalto Max are given, then the function $f(x,y)$ in equation (43) can bereconstructed as follows:

$$\hat{f}_{Max}(x,y) \approx \sum_{p=0}^{Max} \sum_{q=0}^{p} G_{p-q,q}^{(\alpha)} P_{p-q}^{(\alpha)}(x) P_{q}^{(\alpha)}(y) \tag{53}$$

Where the number of moments used in this form for image reconstruction is defined in Eq.(12).

3 Overlapping blocks reconstruction using Exact moments

We learnt from the previous chapter, that regardless of the moments used, It is established that the exact momentscomputation can reduce significantly the reconstruction error rate and increase the outcome quality.

Nevertheless, if we consider images with greater sizes, higher order moments are involved and the handling of greater quantity of information is necessary [13]. Hence the moments computation becomes a time consuming procedure.

Nevertheless, if we consider images with greater sizes, higher order moments are involved and the handling of greater quantity of information is necessary [13]. Hence the moments computation becomes a time consuming procedure.

To overcome this limitation, we first proposed an approach using block based reconstruction method: The input image is subdivided into square blocks of pixels of size (k,l),which generates a number of sub-images reconstructed separately. Because sub-image size is smaller, only low moments's order are needed to better describe its content. Thus, this method allows faster computation of image moments.

However, since each block is handled as an independent entity, discontinuities occur at the block boundaries. This is known as the blocking artifact, which is a consequence of the lack of inter block correlation during the reconstruction process.

In order to exploits this inter block correlation, our proposed approach relies on the overlapping concept: We use for each block the three adjacent neighboring information's by performing the moments computation process on the Overlapped blocks and reconstructing the initial non-overlapped block. In our case, the blocking artifact is dealt with at the source, namely, the moments computation process.

We applied this Overlapping approach to each of the four moments types: Legendre, Zernike, Pseudo-Zernike and Gegenbauer. Hence, we will propose four reconstruction methods:

OBRELM: Overlapping Block based Reconstruction using Exact Legendre Moments.

OBREZM: Overlapping Block based Reconstruction using Exact Zernike Moments.

OBREPZM: Overlapping Block based Reconstruction using Exact Pseudo- Zernike Moments.

OBREGM: Overlapping Block based Reconstruction using Exact Gegenbauer Moments.

Those methods are performed through two stages: (i) the exact moments computation which extracts the block neighborhood information by proceeding on overlapped blocks; (ii) the reconstruction process which acts on output blocks and merge them into the final image (Figure. 1).

The following figures show the reconstruction stages and the Overlapping scheme.

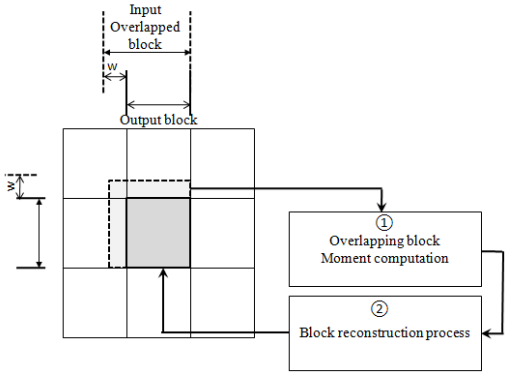

Figure 1 The overlapping scheme of Legendre and Gegenbauer moments, which are defined in the unit square

As we can see in Figure. 1 this overlapping scheme uses the information of the tree neighbors block, It's a one side overlapping, the other side will be overlapped with the next block. In the case of Zernike and Pseudo-Zernikemoments, our overlapping method also proceed by partionning the input image into square blocks of size (k, l), which are then mapped on circular blocks (r, θ) parameters [10].

We consider w extra pixel on one side (Figure.1), the pixels of the additional perimeter would be considered in the moment's computation of this block.

Two works [15] and [19], have proved that an overlapping window size of one pixel is the most effective in terms of image quality and time consuming.

By using the overlapping method, the image space will take the following form:

$$\Omega_{\text{Overlap}} = \{x_i, y_j | 0 \le x_i \le M - 1 + w, \qquad 0 \le y_j \le N - 1 + w\} \tag{53}$$

We assume that:

$$\Omega_{\text{Overlap}} = \bigcup_{n_1=0}^{(S_1-1)} \bigcup_{n_2=0}^{(S_2-1)} D_{\text{Overlap}}^{n_1,n_2}. \tag{54}$$

Where the subset $D_{\text{Overlap}}^{n_1,n_2}$ is expressed as:

$$D_{\text{Overlap}}^{n_1,n_2} = \{x_i, y_j | n_2 k \le x_i \le (n_2 + 1)k - 1 + w, n_1 l \le y_j \le (n_1 + 1)l - 1 + w \ \}. \tag{55}$$

Then let the image function associated to each $D_{\text{Overlap}}^{n_1,n_2}$subset be defined as follows:

$$f_{\text{Overlap}}^{n_1,n_2}(x, y) = \left\{ f(x_i, y_j) \middle| x_i, y_j \in D_{\text{0verlap}}^{n_1,n_2} \right\}. \tag{56}$$

This gives:

$$f(x, y) = \bigcup_{n_1=0}^{(S_1-1)} \bigcup_{n_2=0}^{(S_2-1)} f_{\text{Overlap}}^{n_1,n_2}(x, y) \ . \tag{57}$$

We introduce The Legendre moments defined on the subspace $D_{\text{Overlap}}^{n_1,n_2}$for the Overlapping Block based Reconstruction using Exact Legendre Moments method (OBRELM) is:

$$L_{p,q,Olap}^{E,n_1,n_2} = \sum_{i=n_2k}^{(n_2+1)k-1+w} \sum_{j=n_1l}^{(n_1+1)l-1+w} I_{p,Olap}^{n_1}(x_i)\, I_{q,Olap}^{n_2}(y_j) f^{n_1,n_2}(x_i, y_j) \tag{58}$$

The Zernike moments defined for the Overlapping Block based Reconstruction using Exact Zernike Moments method (OBREZM) is:

$$Z_{pq,Overlap}^{E,n_1,n_2} = \frac{p+1}{\pi} \sum_{\substack{k=|q| \\ p-k=even}}^{p-2} B_{p|q|k} Rad_{kq,Overlap}^{n_1,n_2}. \tag{59}$$

The Pseudo-Zernike moments defined for the Overlapping Block based Reconstruction using Exact Zernike Moments method (OBREPZM) is:

$$PZ_{pq,Ovlap}^{n_1,n_2} = \frac{p+1}{\pi} \left(\sum_{\substack{k=q \\ k-q=even}}^{p} B_{p;q;k} R_{k,q}^{G,n_1,n_2} + \sum_{\substack{k=q+1 \\ k-q=odd}}^{p} B_{p;q;k} R_{k,q}^{H,n_1,n_2} \right),. \tag{60}$$

The Gegenbauer moments defined for the Overlapping Block based Reconstruction using Exact Gegenbauer Moments method (OBREGM) is:

$$G_{p,q,Ovlap}^{E,n_1,n_2} = \frac{1}{C_p(\alpha) C_q(\alpha)} \sum_{i=n_2k}^{(n_2+1)k-1+w} \sum_{j=n_1l}^{(n_1+1)l-1+w} IX_{p,Olap}^{n_1}(x_i)\, IY_{q,Olap}^{n_2}(y_j) f^{n_1,n_2}(x_i, y_j). \tag{61}$$

Then, the functions of each image block using the OBRELM, OBREZM, OBREPZM and OBREGM are as follows:

$$\hat{f}_{max,Ovlap}^{n_1,n_2}(x_i, y_j) \approx \sum_{p=0}^{max} \sum_{q=0}^{p} L_{p-q,q,Ovlap}^{E,n_1,n_2} P_{p-q,Ovlap}(x_i) P_{q,Ovlap}(y_j). \tag{62}$$

$$\hat{f}_{max,Ovlap}^{n_1,n_2}(x_i, y_j) \approx \sum_{p=0}^{max} \sum_{\substack{q \\ p-q=even \\ q \le p}}^{p} \lambda_p Z_{p,q,Ovlap}^{E,n1,n2} V_{p,q}^{n1,n2}(x_i, y_j). \tag{63}$$

$$\hat{f}_{max,Ovlap}^{n_1,n_2}(x_i, y_j) \approx \sum_{p=0}^{max} \sum_{\substack{q \\ p-q=even \\ q \le p}}^{p} \lambda_p Z_{p,q,Ovlap}^{E,n1,n2} V_{p,q}^{n1,n2}(x_i, y_j). \tag{64}$$

$$\hat{f}^{n_1,n_2}_{max,Ovlap}(x_i, y_j) \approx$$

$$\sum_{p=0}^{max}\sum_{q=0}^{p} G^{E,n_1,n_2}_{p-q,q,Ovlap} P_{p-q,Ovlap}(x_i) P_{q,Ovlap}(y_j).$$

The image function up to max of the three approaches using Legendre, Zernike and Gegenbauer moments can be finally obtained by:

$$\hat{f}_{max}(x,y) = \bigcup_{n_1=0}^{(S_1-1)} \bigcup_{n_2=0}^{(S_2-1)} \hat{f}^{n_1,n_2}_{max,Overlap}(x,y), \quad (66)$$

Our approaches OBRELM, OBREZM, OBREPZM and OBREGM using respectively Legendre, Zernike, Pseudo-Zernike and Gegenbauer moments achieve improvement in the following points:

i. Giving high reconstruction quality by using only a small finite number of moments.
ii. Mitigating the artifact involved in the block processing by exploiting the block neighborhood information during the moments computation step, which allows to avoid enhancement post processing techniques which are a time-consuming procedures.

This property can be used to extract local features from the desired Region of interest (ROI). Also, it can be applied in the field of data compression, in which we aim to reconstruct the original image using only a finite number of moments.

4 Applications of our four proposed methodes

4.1 Local features extraction

In this section, we show that we can use our proposed block representation approaches, based on continuous moments, for local features extraction from an image. The local features can be extracted easily from any desired location in the image (region of interest), due to the capability of our approaches to separately represent the information of each block. Consequently, their use in object classification and recognition applications is highly significant. Our proposed local features extraction algorithm is described as follows: firstly; the input image is divided into small blocks. Secondly, for each block that correspond to the desired ROI, we apply our proposed methods (OBRELM, OBREZM, OBREPZM and OBREGM) for extracting the local features. Finally, we transform the resulting moments coefficients to a classifier (Figure 2).

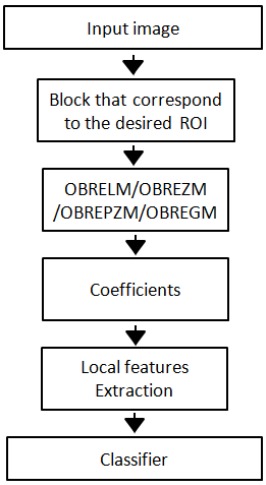

Figure 1 The principe of applying our four approaches in local feature extraction for classification

4.2 Compression algorithm

The compression algorithm is described as follows: Each images is first divided into sub-blocks whose size is (M x M), each block is then transformed by using the OBRELM, OBREZM, OBREPZM and OBREGM. At last, the set of calculated moments are transmitted to the receiver to be used in the reconstruction step (Figure .3) .

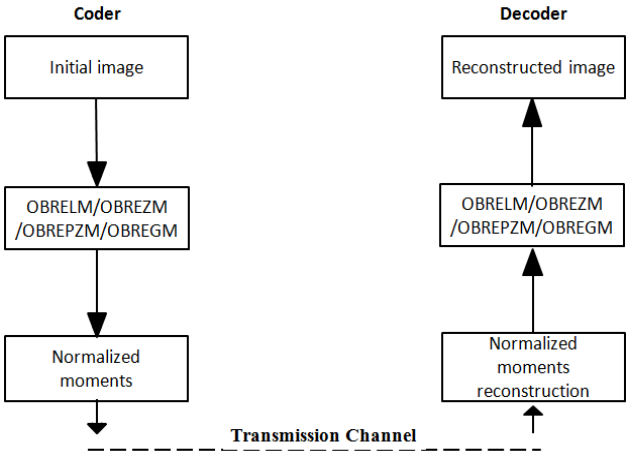

Figure 2 Diagram of encoding/ decoding scheme

In order to evaluate the performance of different methods, we use the total compression ratio [17] which is defined as follows:

$$TCR = \frac{image\ debit}{number\ of\ moments} \tag{67}$$

5 Experimental results

This section aims to prove the effectiveness of the proposed methods using Legendre, Zernike, pseudo-Zernike and Gegenbauer moments in terms of compression rate and local features extraction. Therefore, a (128 x 128) real gray level “clock” test image is used to compare our four proposed methods in terms of local features extraction. In order to complete our study, a comparison of our approaches with DCT for image compression is made in terms of SSIM index, PSNR and time consuming using 128 x 128 Lena image.

5.1 Local features extraction

To measure the capacity of our method, using continuous orthogonal moments, in term of local feature extraction, we have conducted the local sub-image reconstruction via our approaches on a Clock image. Firstly, we reconstruct just the clock object with only small moments orders. Then, we have adopted the Peak Signal-to-Noise ratio (PSNR) and SSIM index [20] as the measurements to evaluate the reconstructed images.

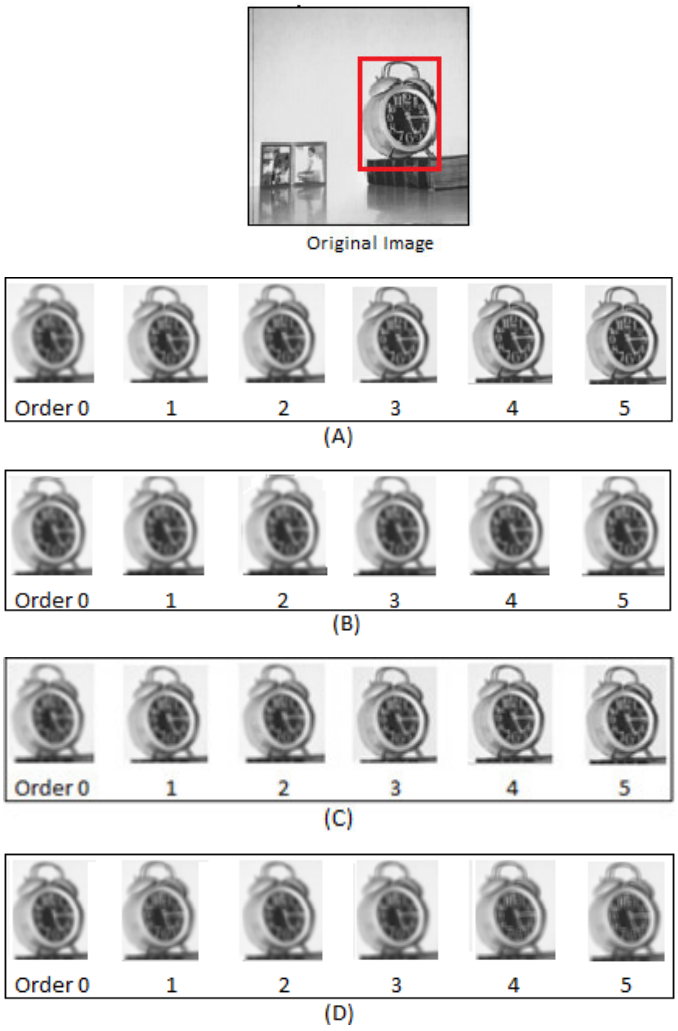

Figure 3 Local Reconstuction image using Overlapping block approaches of Clock image using Legendre moments (OBRELM) (A), Zernike moments (OBREZM) (B),), Pseudo-Zernike moments (OBREPZM) (C) and Gegenbauer moments (OBREGM) (D) with different orders

Tablem 1 Values of the PSNR/SSIM for the local reconstructed clock images using the methods based on overlapping block: OBRELM, OBREZM, OBREPZM and OBREGM using respectively Legendre, Zernike,Pseudo-Zernike and Gegenbauer moments with block size (4x4).

	OBRELM	OBREZM	OBREPZM	OBREGM
Order	PSNR/SSIM			
0	23.55/0.89	23.15/0.88	23.50/0.90	20.77/0.79
1	25.38/0.91	23.48/0.89	25.79/0.90	21.30/0.83
2	27.73/0.94	25.24/0.90	28.02/0.94	22.34/0.89
3	30.05/0.95	27.40/0.92	30.76/0.96	24.39/0.91
4	32.46/0.97	30.95/0.96	33.13/0.98	28.85/0.92
5	33.35/0.99	31.08/0.98	33.56/0.99	30.04/0.94

The above results (Figure.4, Table.1) illustrates the efficiency of the proposed methods against the blocking artifact. They show how a relatively small finite set of moments can adequately characterize the given image with no need to include higher order moments. The OBRELM and OBREPZM perform the best, OBREZM using Zernike moments performs well throughout the reconstruction process and the OBREGM using Gegenbauer moments perform lower than the others.

5.2 Compression: Comparison with DCT

In this section, comparison is made between our approaches and DCT for image compression. The information is stored in some computed moments and coefficients in our three methods and DCT respectively. After reconstruction, the PSNR and SSIM produces by the four methods are compared.

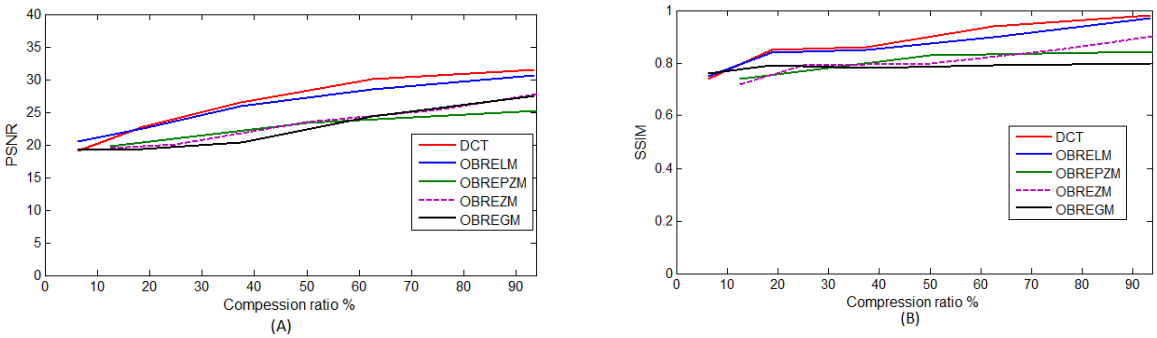

Figure 4 Comparison between OBRELM, OBREZM, OBREGM and DCT for (128 x 128) Lena image using block size (4 x 4) in terms of PSNR (a) and SSIM Index (b)

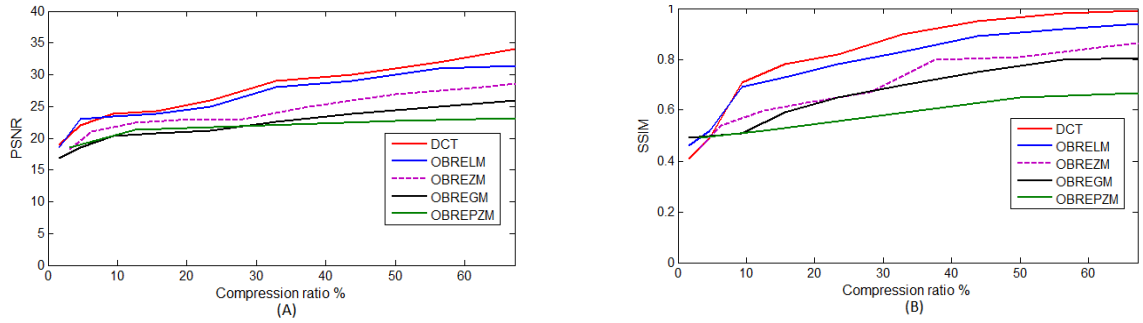

Figure 5 comparison between OBRELM, OBREZM, OBREGM and DCT for (128 x 128) Lena image using block size (8 x 8) in terms of PSNR (a) and SSIM Index (b)

Table 3The reduction factors of reconstruction time for our proposed methods, using 128 x 128 Lena image and (4 x 4) block size, for PSNR = 20, compared to the global reconstruction with 2.0 GHz i7 and 8 GB RAM.

Method	**OBRELM**	**OBREZM**	**OBREPZM**	**OBREGM**
Corresponding moments Order	0	1	0	2
CPU elapsed time	0.064s	1.87s	12.10s	0.58s
Time Reduction	97.58%	92.23%	75.56%	81.62%

The results in Figure. 5 and Figure. 6 indicates that reconstruction using Legendre moments OBRELM provide a better compression capability compared to Zernike, Pseudo-Zernike and Gegenbauer moments which is. Whereas the OBRELM is slightly lower than DCT. However, for high compression rates the performance is almost similar.

For a better compression ratio, a quantification and numerical redundancy exploitation and entropy coding method such as Huffman coding [27] can be used.

Table 2 confirms that the OBRELM is a way better in term of data compression, but also in time reduction. This also means the other methods are unsuitable because the compression schemes require very fast encoding/ decoding image with low time consumption.

The OBRELM is better than the OBREZM and OBREPZM due to the fact that Zernike and Pseudo-Zernike moments are a complex numbers and require, for a given order, two parts in the computation: magnitude and phase. Hence, in the step of Zernike and Pseudo-Zernike moments reconstruction it will need an additional computation of the two values and, by the way, increases the complexity of the overall process. Some works used only magnitude information for recognition but involves erroneous results and impreciseness [28].

6 Conclusion

In this paper, a novel and faster algorithm for the computation of exact continuous moments: Legendre, Zernike, Pseudo-Zernike and Gegenbauer, have been presented. We proved that, by replacing a greater size gray level image by a set of blocks, the moments computation can be accelerated significantly by using only small finite number of moments. We have also applied those methods to local features extraction and to data compression. The experimental results prove that the proposed methods outperforms the conventional ones in terms of error reduction, image quality and time consumption. Our OBREPZM method seems to be the best approach in term of local features extraction but it is high time consuming. In the other hand, our OBRELM method is the most suitable for data compression. Indeed, our approach allows a high compression ratio and deliver a good visual quality and low reconstruction error with less time consuming.

REFERENCES

[1] M. K. Hu, “Visual problem recognition by moment invariant,” IRE Trans. Inform. Theory, vol. IT-8, pp. 179-187, Feb. 1962.

[2] M. Teague, “Image analysis via the general theory of moments,” J. Opt. Soc. Amer., vol. 70, no. 8, pp. 920-930, 1980

[3] C.-H. Teh and R. T. Chin, “On image analysis by the methods of moments,” IEEE Trans. on Pattern Analysis and Machine Intelligence, vol. 10, no. 4, pp. 496–513, 1988.

[4] Krawtchook liao

[5] J. Haddadnia, K. Faez, and P. Moallem, “Neural network based face recognition with moment invariants,” Proceedings of ICIP2001, Thessaloniki, Greece, pp. 1018-1021, 2001.

[6] A. Khotanzad, Y.H. Hong, "Invariant image recognition by Zernike moments", IEEETrans. Pattern Anal. Mach. Intell. 12 (1990) 489–497

[7] R. Luo, T. Lin, Finger crease pattern recognition using Legendre moments and principal component analysis, Chin. Opt. Lett. 5(3), 160–163 (2007).

[8] P.-T. Yap, R. Paramesran, “An efficient method for the computation of Legendre moments,” IEEE Trans. Pattern Anal. Mach. Intell, vol. 27, no. 12, pp. 1996–2002,2005

[9] K.M. Hosny, “Exact Legendre moment computation for gray level images,” Pattern Recognition, vol. 40, no. 12, pp. 3597–3605, 2007.

[10] K.M. Hosny, "Fast computation of accurate Zernike moments", Journal of Real-Time Image Processing 3 (2008) 97–107.

[11] K.M. Hosny, K.M. "Fast computation of accurate Pseudo-Zernike moments for binary and gray-level images". Int Arab J Inf Technol., 2014, 11, (3).

[12] K.M. Hosny, "Image representation using accurate orthogonal Gegenbauer moments". Pattern Recognit. Lett. 2011, 32, (6), pp. 795–804

[13] H. El Fadili, K. Zenkouar and H. Qjidaa, “Lapped block image analysis via the method of Legendre moments,” EURASIP Journal on Applied Signal Processing, vol. 2003, no.9, pp. 902-913, 2003.

[14] Z. Bahaoui, K. Zenkouar, H. El fadili, H.Qjidaa, A.Zarghili, Global overlapping block based reconstruction using exact Legendre moments, CIST (2014), pp. 323 - 328.

[15] Z. Bahaoui, K. Zenkouar, H. El fadili, H.Qjidaa, A.Zarghili, blocking artifact removal using partial overlapping based on exact Legendre moments computation, Journal of Real-Time Image Processing, (DOI :10.1007/s11554-014-0465-3) (2014)1861-8200.

[16] S.G. Mallat, A theory for multiresolution signal decomposition the wavelet representation, IEEE Trans. Pattern Anal. Machine Intel. 11 (7) 1989.

[17] H. Zenkouar, A. Nachit, "Images compression using moments method of orthogonal polynomials", Materials Science and Engineering: B, 49(3), pp. 211–215 (1997)

[18] ISO/IEC 10918-1, Digital compression and coding of continuous-tone still images: requirements and guidelines, February, 1994.

[19] Reeve III, H.C., Lim, J.S.: Reduction of blocking effect in image coding, Proceedings of ICASSP 83, 1212 -1215 (1988).

[20] Z. Wang, A. C. Bovik, H. R. Sheikh, and E. P. Simoncelli, “Image quality assessment: From error visibility to structural similarity,” Image Processing, IEEE Transactions on, 2004, vol. 13, no. 4, pp. 600–612

